

S₁-State Model of the O₂-Evolving Complex of Photosystem II

Sandra Lubner,^{*,†} Ivan Rivalta,[†] Yasufumi Umena,^{||} Keisuke Kawakami,[‡] Jian-Ren Shen,[§] Nobuo Kamiya,[‡] Gary W. Brudvig,[†] and Victor S. Batista^{*,†}

[†]Department of Chemistry, Yale University, New Haven, Connecticut 06520-8107, United States

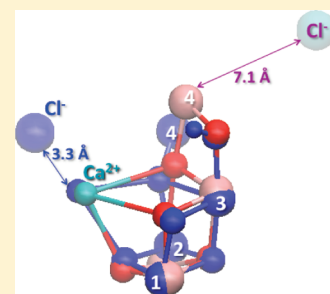
[‡]Department of Chemistry, Graduate School of Science, and The OCU Advanced Research Institute for Natural Science and Technology (OCARINA), Osaka City University, Sumiyoshi, Osaka 558-8585, Japan

[§]Division of Bioscience, Graduate School of Natural Science and Technology/Faculty of Science, Okayama University, 1-1, Naka 3-chome, Tsushima, Okayama 700-8530, Japan

^{||}Institute for Protein Research, Osaka University, 3-2 Yamadaoka, Suita-shi, Osaka 565-0871, Japan

S Supporting Information

ABSTRACT: We introduce a quantum mechanics/molecular mechanics model of the oxygen-evolving complex of photosystem II in the S₁ Mn₄(IV,III,IV,III) state, where Ca²⁺ is bridged to manganese centers by the carboxylate moieties of D170 and A344 on the basis of the new X-ray diffraction (XRD) model recently reported at 1.9 Å resolution. The model is also consistent with high-resolution spectroscopic data, including polarized extended X-ray absorption fine structure data of oriented single crystals. Our results provide refined intermetallic distances within the Mn cluster and suggest that the XRD model most likely corresponds to a mixture of oxidation states, including species more reduced than those observed in the catalytic cycle of water splitting.



Photosystem II (PSII) is a transmembrane protein complex with ~20 protein subunits, several electron-transfer quinone factors, and a photoantenna system of chlorophyll and carotenoid pigments. Of special interest is the oxygen-evolving complex (OEC), which contains a CaMn₄ cluster that catalyzes the oxidation of water to produce dioxygen.^{1–5} In contrast to (electro)chemical water splitting, direct solar water oxidation by the OEC requires only moderate activation energies and features high turnover rates that are still unmatched by artificial water splitting systems. Elucidating its molecular structure is thus an important prerequisite for a detailed understanding of the catalytic cycle and the development of biomimetic catalysts.

A variety of spectroscopic methods have been applied to study the OEC, including mass spectrometry,^{6,7} Fourier transform (FT) infrared spectroscopy,⁸ electron paramagnetic resonance spectroscopy,^{9,10} and X-ray diffraction (XRD).^{11–16} Until recently, XRD data were available only at moderate resolution,^{11–15} leaving uncertainty with respect to the exact position of the manganese atoms, water molecules, and coordination of the surrounding ligands. Nevertheless, tentative OEC models were proposed on the basis of the XRD density maps and high-resolution spectroscopic data. The recent breakthroughs in XRD provide for the first time data at 1.9 Å resolution,^{16,17} suggesting a cuboidal structure similar to previous models, although with a ligation scheme in which Ca²⁺ is bridged to Mn centers by the carboxylate moieties of D170 and A344 centers (see Figure 1). These results offer a great opportunity to establish a structural model of the OEC in the resting or so-called storage state

(S state), S₁. Such a model should be particularly valuable for understanding the catalytic mechanism of water splitting in PSII.

Previous studies have proposed high-resolution extended X-ray absorption fine structure (EXAFS) measurements to rule out structural models of the OEC that did not match the isotropic and crystal orientation-dependent polarized data.^{18,19,22} In addition, several models of the OEC core, which are consistent with experimental EXAFS spectra, have been proposed.²² Moreover, complete models, including the coordination of surrounding ligands on the basis of the 1SSL crystal structure,¹³ have also been shown to agree with EXAFS data. In fact, it has been possible to derive OEC models from quantum mechanics/molecular mechanics (QM/MM) calculations using density functional theory (DFT)^{23–25} for the S-state intermediates along the catalytic cycle, S₀, S₁, S₂, S₃, and S₄. In addition, an S₁-state model matching polarized experimental EXAFS data has been obtained by refining the structure of the optimized QM/MM model.²³ This has been achieved by minimizing a score function based on the root-mean-square deviations of the experimental and calculated polarized EXAFS spectra. The resulting refinement could also be achieved by QM optimization biased by deviations between simulated and experimental EXAFS spectra.²⁶ Here, we report for the first time the analogous

Received: May 3, 2011

Revised: June 14, 2011

Published: June 16, 2011

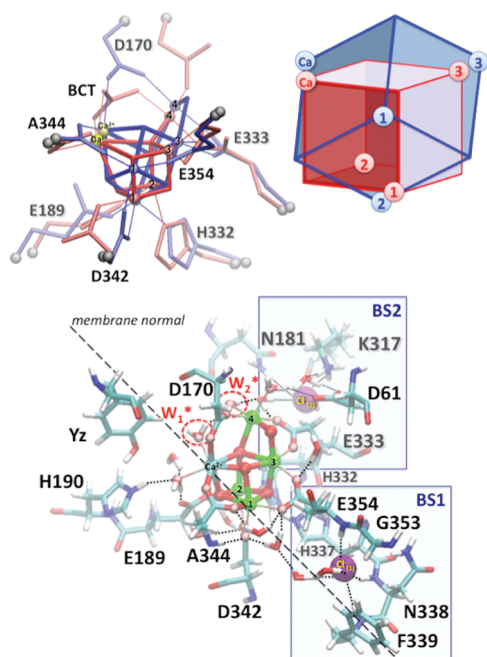


Figure 1. Superposition of the OEC in the X-ray models of PSII at 1.9 Å (blue)^{16,17} and 3.5 Å (red)¹³ resolution (top). Ligation scheme with D170 bridging between Mn(4) and Ca, and chloride binding sites (BS1 and BS2) as proposed by the X-ray model at 1.9 Å resolution (bottom).

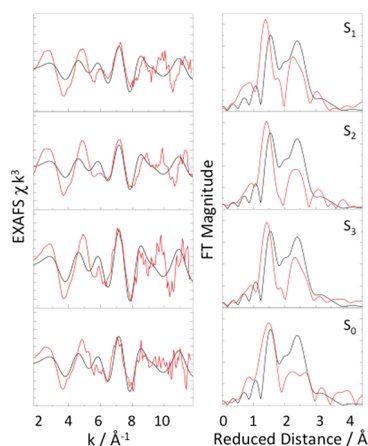


Figure 2. Comparison between experimental (red)^{19,20} k^3 -weighted EXAFS spectra (left) and Fourier transform (FT) magnitudes (right) for the OEC of PSII in the S₀–S₃ states and the simulated (black) spectrum for the new X-ray model (chain A) at 1.9 Å resolution. Reduced space spectra show prominent peaks corresponding to scattering centers in the first (O and N), second (Mn in the core), and third (dangling Mn, and Ca) coordination shells of Mn.

DFT-QM/MM model based on the ligation scheme determined by the new X-ray model as well as its EXAFS-refined structure. The DFT-QM/MM model is built by using the two-layer ONIOM link hydrogen atom approach, implemented in Gaussian 09,²⁷ as in our previous studies.^{23–25} The preparation of the initial electronic state is based on high-quality spin-electronic states for the ligated cluster of Mn ions using Jaguar version 7.7.²⁸ Geometry-optimized structures were obtained under the constraint of fixed α -carbon atoms (for details, see the Supporting Information)

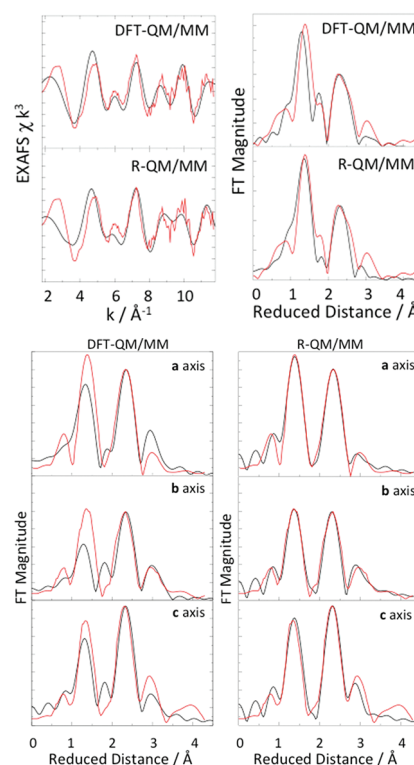


Figure 3. Comparison between experimental (red)^{19,20,22} and calculated (black) isotropic (top two rows) and polarized (bottom three rows) EXAFS spectra for the OEC of PSII in the S₁ state calculated from the new DFT-QM/MM and refined R-QM/MM model.

as determined by the coordinates in the new XRD model. EXAFS spectra were calculated using the ab initio real space Green function approach in FEFF (version 8.30), employing the coordinates of the Mn₄Ca cluster and surrounding ligands provided by the model system of interest.

Figure 2 shows that the isotropic EXAFS spectrum calculated for the new XRD model is significantly different from the experimental spectrum^{19,20} of the S₁ state. This is likely due to the fact that the XRD model does not have any Mn–Mn distance shorter than 2.8 Å in chain A. While the comparison to the S₀ state is more favorable, there is no quantitative agreement with any S-state intermediate. This could be due to reductive damage caused by the high doses of X-ray radiation,²¹ leading to a mixture of reduced S states, or simply structural disorder (in the absence of radiation damage for PSII crystallized as a mixture of S-state intermediates along the catalytic cycle). While the former possibility is likely to be the case, the latter is ruled out via comparison of the calculated spectrum of the XRD model to weighted averages of experimental S₀, S₁, S₂, and S₃ spectra (see the Supporting Information). Even mixtures with the best possible fit (e.g., including ~60% of the S₀ intermediate) do not generate average spectra in quantitative agreement with the spectrum of the XRD model. These results suggest that the coordinates of the new X-ray model do not correspond to any S₀–S₃ intermediate, or mixture of solely those intermediate states, but may contain also pre-S₀-state intermediates such as S_{–1} and S_{–2}. Other causes may be experimental errors (0.16 Å) in the XRD model as well as a different combination of spin states of the metal ions and protonation states of the ligands.

Table 1. Intermetallic Distances (Å) in the X-ray Model (chain A/a),¹⁶ Compared to Those from the New DFT-QM/MM Model Obtained with the B3LYP (BP86) Density Functional, the Refined R-QM/MM Model, and the 2006 DFT-QM/MM Model²⁵

	X-ray A/a	QM/MM B3LYP (BP86)	R-QM/ MM	2006-QM/ MM
Mn(1)–Mn(2)	2.84/2.76	2.80 (2.81)	2.76	2.76
Mn(1)–Mn(3)	2.89/2.91	2.80 (2.80)	2.71	2.76
Mn(2)–Mn(3)	3.29/3.30	3.38 (3.38)	3.25	2.82
Mn(3)–Mn(4)	2.97/2.91	2.75 (2.74)	2.76	3.72
Mn(2)–Mn(4)	5.00/4.95	4.89 (4.88)	4.68	3.34
Ca–Mn(2)	3.51/3.46	3.56 (3.52)	3.52	3.31
Ca–Mn(3)	3.41/3.44	3.62 (3.59)	3.49	3.95
Ca–Mn(1)	3.36/3.29	3.35 (3.36)	3.38	3.59
Ca–Mn(4)	3.79/3.80	3.81 (3.77)	3.67	3.84

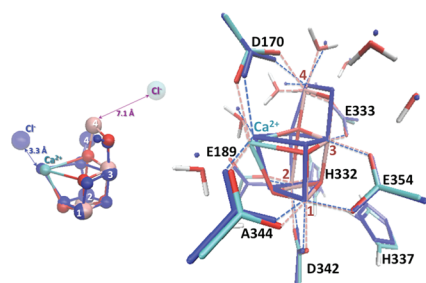


Figure 4. Comparison of the new DFT QM/MM model of the OEC of PSII in the S₁ state (colors) and the 2006 DFT QM/MM model (blue) (left). X-ray model at 1.9 Å resolution (blue) and the new DFT-QM/MM model (colors) (right).

Figure 3 shows the experimental isotropic^{19,20} and polarized²² EXAFS spectra for the S₁ state, as compared to the corresponding spectra calculated for the DFT-QM/MM model of the OEC. This model is based on the new XRD model, in which the dangling Mn(4) is bridged to Ca by the carboxylate moiety of D170. The oxidation state Mn₄(IV,III,IV,III) is predicted with the BP86^{29,30} and B3LYP^{31,32} density functionals. Intermetallic distances, listed in Table 1, and Mulliken atomic spin densities [−2.9 and −2.7 for Mn(1), 3.9 and 3.8 for Mn(2), 2.9 and 2.6 for Mn(3), and −3.9 and −3.6 for Mn(4), respectively (for numbering of atoms, see Figure 1)] are consistent with high-resolution spectroscopy. The resulting model gives isotropic and polarized EXAFS spectra in good agreement with experimental data. The directly bound ligands (D170, A344, E189, E354, E333, and D342) and μ -oxo bridges are unprotonated, while all water ligands are H₂O (compare the left-hand side of Figure 4 for a picture of the DFT-QM/MM model obtained with the B3LYP density functional).

To obtain a model of the OEC in quantitative agreement with high-resolution spectroscopic data, we implemented an EXAFS structural refinement scheme as reported previously.²³ We refined the DFT-QM/MM model by iteratively adjusting the nuclear coordinates to minimize a scoring function defined as the sum of the squared deviations between calculated and experimental EXAFS spectra, plus a quadratic penalty factor that ensures minimum displacements of the nuclear positions relative to the reference configuration. As shown in Figure 3, the resulting

configuration of the R-QM/MM model yields isotropic and polarized EXAFS data in quantitative agreement with experiments. As mentioned in previous work,²³ however, the agreement with high-resolution spectroscopic data does not rule out other possible structures because the model is a local solution relative to the reference DFT-QM/MM structure. The comparison of the cuboidal structure of the OEC in the new DFT-QM/MM model (obtained from the B3LYP density functional) and the 2006 DFT-QM/MM model²⁵ based on the XRD model at 3.5 Å resolution is shown in Figure 4, and the complete comparison of intermetallic distances in the models of the OEC of PSII is reported in Table 1, including the new XRD structure at 1.9 Å resolution, the new DFT-QM/MM model of the OEC in the S₁ state, the new R-QM/MM model, and the 2006 DFT-QM/MM structure. While there are similarities among the various models, there are also significant differences, including the new D170 bridge between Ca and Mn(4), shortening the Mn(3)–Mn(4) and elongating the Mn(2)–Mn(3) distances when compared to those in the 2006 DFT-QM/MM structure.

In summary, we have introduced a DFT-QM/MM model of the OEC of PSII in the S₁ Mn₄(IV,III,IV,III) state, with a ligation scheme consistent with the new XRD model, where Ca²⁺ is bridged to Mn centers by the carboxylates of D170 and A344. In contrast to the XRD model, the DFT-QM/MM structure is fully consistent with high-resolution spectroscopic data, including polarized EXAFS spectra of oriented single crystals, suggesting that the XRD model corresponds to a mixture of states, most likely including S₀ and pre-S₀ intermediates S_{−1} and S_{−2}. The revised DFT-QM/MM structure should be particularly relevant to the analysis of S-state intermediates, consistent with the ligation scheme proposed by the new XRD model.

■ ASSOCIATED CONTENT

S Supporting Information. Description of computational methods. This material is available free of charge via the Internet at <http://pubs.acs.org>.

■ AUTHOR INFORMATION

Corresponding Authors

*E-mail: sandra.luber@yale.edu or victor.batista@yale.edu. Phone: (203) 432-6672. Fax: (203) 432-6144.

Funding Sources

V.S.B. acknowledges financial support from the Division of Chemical Sciences, Geosciences, and Biosciences, Office of Basic Energy Sciences, U.S. Department of Energy (DE-SC 000-1423), supercomputer time from National Energy Research Scientific Computing, and support from National Institutes of Health (NIH) grants GM84267 and GM043278 for the development of methods implemented in this study. G.W.B. acknowledges support from NIH Grant GM32715.

■ REFERENCES

- (1) McEvoy, J. P., and Brudvig, G. W. (2006) *Chem. Rev.* 106, 4455–4483.
- (2) Diner, B. A., and Babcock, G. T. (1996) in *Oxygenic photosynthesis: The light reactions*, pp 213–247, Kluwer Academic Publishers, Dordrecht, The Netherlands.
- (3) Britt, R. D. (1996) in *Oxygenic photosynthesis: The light reactions*, pp 137–164, Kluwer Academic Publishers, Dordrecht, The Netherlands.

- (4) Witt, H. (1996) *Ber. Bunsen-Ges.* 100, 1923–1942.
- (5) Debus, R. J. (1992) *Biochim. Biophys. Acta* 1102, 269–352.
- (6) Hillier, W., and Wydrzynski, T. (2004) *Phys. Chem. Chem. Phys.* 6, 4882–4889.
- (7) Messinger, J., Badger, M., and Wydrzynski, T. (1995) *Proc. Natl. Acad. Sci. U.S.A.* 92, 3209–3213.
- (8) Chu, H., Hillier, W., and Debus, R. (2004) *Biochemistry* 43, 3152–3166.
- (9) Peloquin, J., Campbell, K., Randall, D., Evanchik, M., and Pecoraro, V. et al. (2000) *J. Am. Chem. Soc.* 122, 10926–10942.
- (10) Kulik, L., Epel, B., Lubitz, W., and Messinger, J. (2005) *J. Am. Chem. Soc.* 127, 2392–2393.
- (11) Biesiadka, J., Loll, B., Kern, J., Irrgang, K., and Zouni, A. (2004) *Phys. Chem. Chem. Phys.* 6, 4733–4736.
- (12) Kamiya, N., and Shen, J. (2003) *Proc. Natl. Acad. Sci. U.S.A.* 100, 98–103.
- (13) Ferreira, K. N., Iverson, T. M., Maghlaoui, K., Barber, J., and Iwata, S. (2004) *Science* 303, 1831–1838.
- (14) Loll, B., Kern, J., Saenger, W., Zouni, A., and Biesiadka, J. (2005) *Nature* 438, 1040–1044.
- (15) Guskov, A., Kern, J., Gabdulkhakov, A., Broser, M., and Zouni, A. et al. (2009) *Nat. Struct. Mol. Biol.* 16, 334–342.
- (16) Umena, Y., Kawakami, K., Shen, J.-R., and Kamiya, N. (2011) *Nature* 473, 55–60.
- (17) Kawakami, K., Umena, Y., Kamiya, N., and Shen, J.-R. (2011) *J. Photochem. Photobiol., B* 104, 9–18.
- (18) Grabolle, M., Haumann, M., Muller, C., Liebisch, P., and Dau, H. (2006) *J. Biol. Chem.* 281, 4580–4588.
- (19) Haumann, M., Muller, C., Liebisch, P., Iuzzolino, L., and Dittmer, J. et al. (2005) *Biochemistry* 44, 1894–1908.
- (20) Dau, H., Liebisch, P., and Haumann, M. (2004) *Phys. Chem. Chem. Phys.* 6, 4781–4792.
- (21) Yano, J., Kern, J., Irrgang, K., Latimer, M., and Bergmann, U. et al. (2005) *Proc. Natl. Acad. Sci. U.S.A.* 102, 12047–12052.
- (22) Yano, J., Kern, J., Sauer, K., Latimer, M. J., and Pushkar, Y. et al. (2006) *Science* 314, 821–825.
- (23) Sproviero, E. M., Gascon, J. A., McEvoy, J. P., Brudvig, G. W., and Batista, V. S. (2008) *J. Am. Chem. Soc.* 130, 6728–6730.
- (24) Sproviero, E. M., Gascon, J. A., McEvoy, J. P., Brudvig, G. W., and Batista, V. S. (2008) *J. Am. Chem. Soc.* 130, 3428–3442.
- (25) Sproviero, E. M., Gascon, J. A., McEvoy, J. P., Brudvig, G. W., and Batista, V. S. (2006) *J. Chem. Theory Comput.* 2, 1119–1134.
- (26) Hsiao, Y.-W., Tao, Y., Shokes, J. E., Scott, R. A., and Ryde, U. (2006) *Phys. Rev. B* 74, 214101.
- (27) Frisch, M. J., Trucks, G. W., Schlegel, H. B., Scuseria, G. E., Robb, M. A., et al. (2009) *Gaussian 09*, Gaussian, Inc., Wallingford, CT.
- (28) *Jaguar*, version 7.7 (2010) Schroedinger, LLC, New York.
- (29) Becke, A. D. (1988) *Phys. Rev. A* 38, 3098–3100.
- (30) Perdew, J. P. (1986) *Phys. Rev. B* 33, 8822–8824.
- (31) Becke, A. D. (1993) *J. Chem. Phys.* 98, 5648–5652.
- (32) Lee, C., Yang, W., and Parr, R. G. (1988) *Phys. Rev. B* 37, 785–789.